Polymer 50 (2009) 3950–3954

Contents lists available at ScienceDirect

Polymer

journal homepage: www.elsevier.com/locate/polymer

Influence of alkali metal counterions on the charging behavior of poly(acrylic acid)

Amin Sadeghpour, Andrea Vaccaro, Samuel Rentsch [1], Michal Borkovec*

Department of Inorganic, Analytical, and Applied Chemistry, University of Geneva, Sciences II, 30, Quai Ernest-Ansermet, CH-1211 Geneva 4, Switzerland

ARTICLE INFO

Article history:
Received 1 May 2009
Received in revised form
14 June 2009
Accepted 17 June 2009
Available online 21 June 2009

Keywords:
Polyelectrolyte
Titration
Poly(acrylic acid)

ABSTRACT

Charging of poly(acrylic acid) (PAA) in the presence of different alkali metal counterions was studied by precision potentiometric titration. The charging behavior can be described with a novel cylinder Stern model quantitatively. This model is based on the Poisson–Boltzmann equation in the cylinder geometry and a constant Stern capacitance. One finds an increasing cylinder radius with increasing mass of the alkali metal ion and a correspondingly decreasing Stern capacitance. The intrinsic ionization constants for the uncharged polymer are found to decrease with ionic strength, similarly to weak acids of low molecular mass.

1. Introduction

Poly(acrylic acid) (PAA) ranks among the most widely used polyelectrolytes in industry, and its key applications include water-treatment and fabrication of super-absorbing materials [1]. PAA interacts with the water–calcite interface very strongly, and it was shown that it can be used to control the precipitation of calcium carbonate [2] and the flow properties of the corresponding slurries [3,4].

PAA is a weak anionic polyelectrolyte whereby the ionization of carboxylic groups is responsible for the buildup of negative charge according to the reaction

$$-\mathrm{COOH} \rightleftharpoons -\mathrm{COO}^- + \mathrm{H}^+ \qquad (1)$$

This characteristic feature of PAA was explored in the fabrication of pH responsive multilayer capsules or brushes [5–8]. PAA brushes swell with progressive ionization, and this process was investigated with colloidal particles with dynamic light scattering [9] and with ellipsometry or reflection spectroscopy on planar substrates [5,8].

The charging process of PAA can be studied by potentiometric titrations in a straightforward way, and for this polyelectrolyte such studies were already carried out many decades ago [10–19]. The data reveal that electrostatic interactions between ionizable groups broaden the charging curves with respect to the monoprotic analog. However, these interactions are not sufficiently strong to induce the two-step charging behavior observed for more highly charged polyelectrolytes, such as poly(maleic acid), poly(fumaric acid), or linear poly(ethylene imine) [15,20–23]. Some authors have suggested that the charging behavior of PAA can be modeled with a Poisson–Boltzmann (PB) cylinder model [12–15], while others proposed that a Debye–Hückel (DH) description is sufficient, provided conformational degrees of freedoms are taken into account [24,25]. Indeed, swelling of PAA with increasing pH was reported recently [26].

Detailed comparison with models makes little sense with experimental data of moderate precision. Titration data for PAA available in literature are seldom obtained at a sufficiently high dilution such that the presence of the counterions of the polyelectrolyte could be neglected with respect to the electrolyte added. Moreover, the charging plateaus were sometimes poorly assigned. The latter aspect is particularly important when the titration data are presented as effective ionization constants pK_{eff} obtained with the Henderson–Hasselbalch equation [15]

$$\mathrm{pH} = pK_{\mathrm{eff}} + \log\frac{\alpha}{1-\alpha} \qquad (2)$$

where α is the degree of ionization ($0 \le \alpha \le 1$). The representation of pK_{eff} is extremely sensitive even to small errors in the charging plateaus near the limiting values of α, which lead to typical spurious upturns or downturns in the pK_{eff} plot.

The monoprotic case is recovered when pK_{eff} corresponds to the constant ionization constant of the respective acid or base. For weak

* Corresponding author. Tel.: +41 22 379 6405.
E-mail address: michal.borkovec@unige.ch (M. Borkovec).
[1] Present address: Omya Development AG, Baslerstrasse 42, CH-4665 Oftringen, Switzerland.

0032-3861/$ – see front matter © 2009 Elsevier Ltd. All rights reserved.
doi:10.1016/j.polymer.2009.06.032

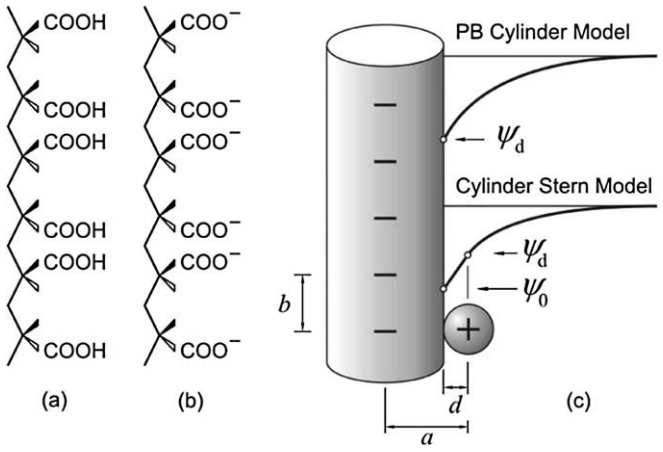

Fig. 1. Structural formulas of (a) protonated and (b) deprotonated syndiotactic poly(acrylic acid) (PAA). (c) Schematic representation of the PB cylinder model and the cylinder Stern model with the corresponding potential profiles.

polyacids, however, pK_{eff} typically increases with increasing α. In the case of poly(methacrylic acid) and poly(ethacrylic acid), however, one observes an intermediate maximum and minimum, and this feature has been suggested to be related to conformational transitions within the chain [12,27–29]. Since this feature is missing in PAA titration, one must expect that its charging behavior is weakly influenced by the conformational change and only dictated by short range interactions along the chain. Counterions may further influence the charging behavior of polycarboxylates substantially [10,21], but these effects have been hardly studied systematically.

We have therefore chosen to reinvestigate the charging behavior of PAA with potentiometric titration. With modern instrumentation, it is straightforward to obtain accurate data at high dilution of the polyelectrolyte, and therefore a wide range of ionic strengths can be investigated. At the same time, we have addressed the charging behavior with different alkali metal cations. We find that the classical PB cylinder model does not always describe the charging behavior properly, but the presently proposed cylinder Stern model is adequate (Fig. 1). These two models are analogous to the diffuse layer model and the basic Stern model in the planar geometry used in the context of water–oxide interfaces [15,30]. We describe a novel characteristic trend of the charging data upon variation of the type of the alkali metal ion.

2. Experimental

Monodisperse PAA has been obtained from Polymer Source in the acidic form. The number weighted molecular mass is 88 kg/mol while its mass weighted average is 99 kg/mol. The similarity of these two numbers confirms the low polydispersity of the sample. According to the manufacturer, the polymer is not branched and mainly syndiotactic (Fig. 1). Hydrochloric acid was from Titrisol (Merck) and CO_2-free sodium hydroxide from Mallinckrodt (Baker). Analytical grade solids LiCl and KCl were obtained from Acros Organics, CsCl and RbCl from Sigma–Aldrich, and NaCl from Fluka. All solutions were prepared by using CO_2-free boiled Milli-Q water.

Titrations were carried out with a home-built instrument using four automatic burets containing 0.25 M HCl, 0.25 M CO_2-free NaOH (Baker Dilut-It), 3.0 M MeCl, and pure water, where MeCl is the respective alkali metal chloride salt. A high-impedance voltmeter was used to measure the potential between a glass electrode and a separate Ag/AgCl reference electrode. The titration vessel was thermostated to 25 °C and it was continuously flushed with moist CO_2-free nitrogen gas. For each titration, about 10 mg of PAA were dissolved in 100 mL of water and titrated at constant ionic strengths from pH 3.5 to 9 and back. The ionic strength was increased with the respective salt after such a run, and the procedure was started all over. Blank titrations were used to calibrate the electrodes and to determine the precise concentration of the base. The charging curves were obtained by subtracting the measured curve from the blank titration. While the PAA solution always contained traces of Na^+, the alkali ion in question was always in excess by at least a factor of 4 even at the lowest ionic strength of 0.005 M. At this ionic strength, the salt concentration was equally larger by a factor of 4 than the concentration of the carboxylic groups from PAA. Therefore, effects of interactions between the polymer chains can be safely neglected at the concentrations used. This point was verified by repeating some titrations at lower PAA concentrations. Plateau values needed for the conversion of titrated charge to the degree of ionization were chosen carefully. Good reproducibility of the procedure was checked by multiple runs. Details on the technique are given elsewhere [15,31].

3. Results and discussion

Charging data of PAA at constant ionic strength in LiCl electrolyte are shown in Fig. 2a. The good agreement between forward and backward titrations confirms the full reversibility of the system. The dependence of the degree of dissociation on pH is weaker than what one would expect for the monomeric unit, as indicated for $pK = 4.5$. The charging curves broaden with decreasing ionic strength, suggesting the increasing importance of electrostatic interactions. Such trends were reported for PAA and other polyacids earlier [12,15,27].

Such data are commonly plotted as the effective ionization constant pK_{eff} defined in Equation (2). This representation shown in Fig. 2b emphasizes the differences between similar titration curves. The solid lines are fits to the data with the cylinder Stern model, which represents a simple generalization of the classical PB cylinder model for polyelectrolytes [12–15]. This model is analogous to the basic Stern model used to model charging behavior of water–oxide interfaces. Such an approach suggests that pK_{eff} can be decomposed into a chemical and an electrostatic contribution according to

$$pK_{eff} = pK - \beta e\psi_0/\ln 10 \tag{3}$$

where pK is the intrinsic ionization constant of the carboxylic group, ψ_0 is the electrostatic surface potential, e is the elementary charge, and β denotes the inverse thermal energy. The charge–potential relation is found by numerically solving the PB equation in cylinder geometry

$$\frac{1}{r}\frac{d}{dr}\left(r\frac{d\psi}{dr}\right) = \frac{\kappa^2}{\beta e}\sinh(\beta e\psi) \tag{4}$$

for the radial potential profile $\psi(r)$ where r is the distance from the cylinder axis and κ is the inverse Debye length given by $\kappa^2 = 2\beta e^2 I N_A/(\varepsilon_0\varepsilon)$ whereby I is the ionic strength of the electrolyte solution, N_A the Avogadro's number, and $\varepsilon_0\varepsilon$ is the dielectric permittivity of water, whereby the value of $\varepsilon = 79$ has been used. The diffuse layer potential is given by $\psi_d = \psi(a)$ where a is the cylinder radius, and the surface charge density is obtained from

$$\sigma = \varepsilon_0\varepsilon\frac{d\psi}{dr}\Big|_{r=a} = -\frac{2\pi e a}{b}\alpha \tag{5}$$

This quantity is related to the degree of dissociation α and to the line charge density e/b, where b corresponds to the mean distance between the charges in the axial direction. The Stern model

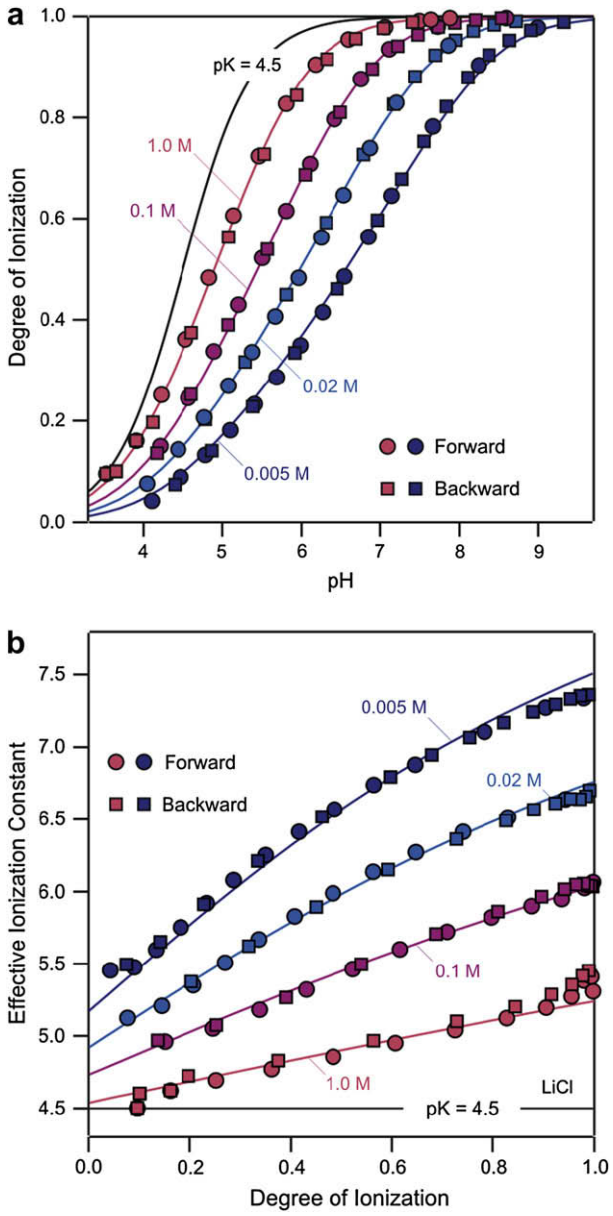

Fig. 2. Potentiometric titrations of poly(acrylic acid) (PAA, top) with LiCl as electrolyte at different ionic strengths. Experimental data (points) are compared with model calculation (lines). The corresponding result for a monoprotic acid with p$K = 4.5$ is given for comparison. (a) Degree of ionization α as a function of pH with forward and backward titrations indicated. (b) Effective ionization constant pK_{eff} as a function of degree of ionization α.

stipulates a simple proportionality relation between the surface charge density and the potential drop of this layer, namely

$$\frac{\sigma}{\psi_0 - \psi_d} = C_S \tag{6}$$

where C_S is the Stern capacitance. The classical PB cylinder model is recovered for $C_S \to \infty$.

These equations are solved self-consistently whereby the adjustable parameters are the cylinder radius a, the mean axial distance between the charges b, the Stern capacitance C_S, and the intrinsic ionization constant pK. We have fixed the axial distance to the value of $b = 0.5$ nm. For each counterion, the cylinder radius and the Stern capacitance are adjusted to one common value for all ionic strengths, while the pK must be adjusted for each ionic strength separately. The best fit to the data is found by a least-squares procedure and is represented by the solid lines in Fig. 2.

The experimental data for the other alkali metal salts together with the corresponding fits are shown in the following figures. Fig. 3 shows the data for NaCl and KCl, while Fig. 4 for RbCl and CsCl. For the data shown in Fig. 4, the titrations at 1 M were not reversible, probably due to the formation of precipitates. The resulting fit parameters of the basic Stern model are summarized in Table 1, while the intrinsic ionization constants pK for the uncharged polymer are given in Table 2. The fitted parameters are equally presented graphically in Fig. 5. When comparing the evolution of the titration curves from the light to the heavy alkali metal ions, one observes that the light metal ions (i.e., Li^+) show clear curvature in the pK plot, while this curvature is completely missing for the heavy ones (i.e., Cs^+). This trend is reflected in the dependence of the fitted model parameters, especially in the increase of the cylinder radius and the decrease of the Stern

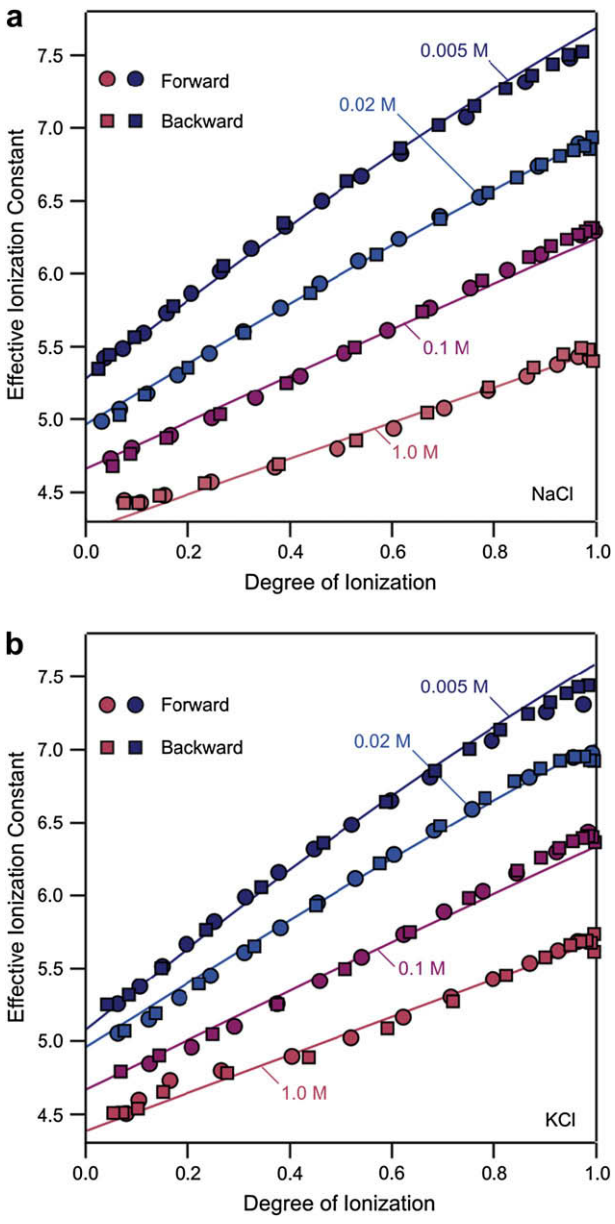

Fig. 3. Potentiometric titration of PAA plotted as effective ionization constant pK_{eff} as a function of degree of ionization α for different ionic strengths. (a) NaCl and (b) KCl.

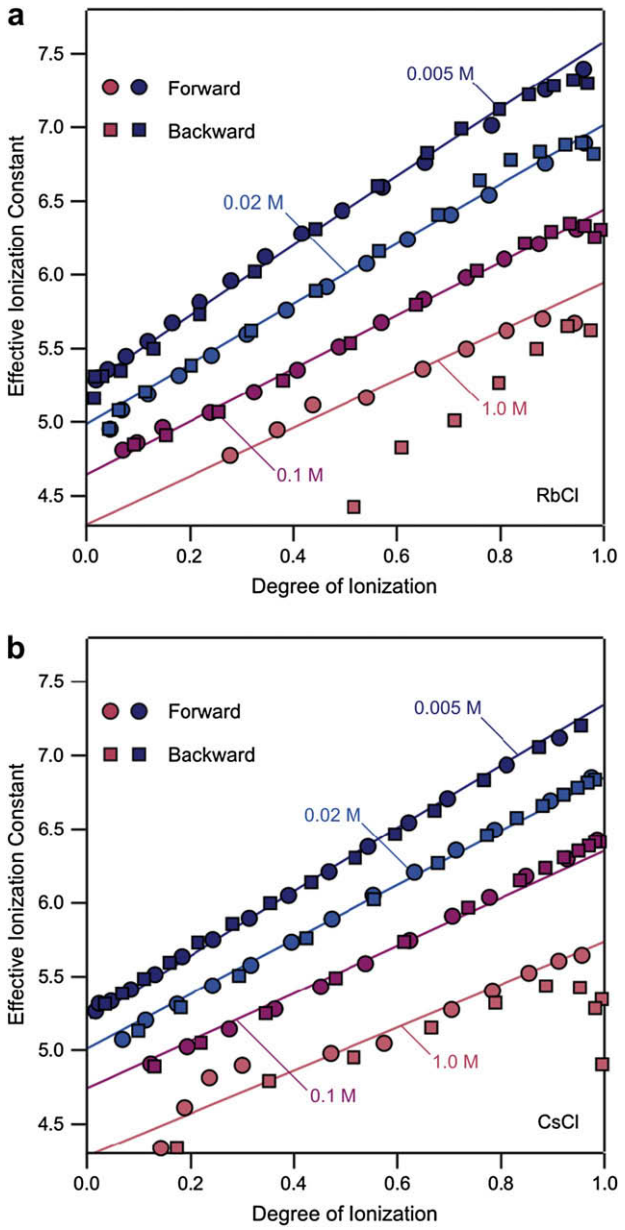

Fig. 4. Potentiometric titration of PAA plotted as effective ionization constant pK_{eff} as a function of degree of ionization α for different ionic strengths. (a) RbCl and (b) CsCl. The titration at the highest ionic strength is not reversible in both cases.

capacitance with increasing mass of the metal ion (Fig. 5a). The effect of interactions between the sites does not vary strongly between the different alkali metal ions, but it decreases slightly with increasing mass of the counterion. A similar, but more pronounce trend was observed for grafted PAA [8].

Only the data with the Li^+ counterion can be well described with the classical PB cylinder model. The fitted Stern capacitance is large, and its precise value has little influence on the quality of the fit. The data set with the Na^+ as the counterion cannot be properly described with the cylinder PB model, and a finite Stern capacitance

Table 1
Fitted parameters of the cylinder Stern model.

	LiCl	NaCl	KCl	RbCl	CsCl
Cylinder radius a (nm)	0.49	1.54	1.43	4.45	4.54
Stern Capacitance C_S (F/m^2)	13.7	0.55	0.56	0.12	0.14

Table 2
Fitted Intrinsic Ionization Constants pK of the Uncharged Polymer.

Ionic strength (M)	LiCl	NaCl	KCl	RbCl	CsCl
0.005	5.17	5.28	5.08	5.25	5.20
0.02	4.92	4.96	4.96	4.99	5.01
0.1	4.73	4.66	4.66	4.64	4.74
1	4.54	4.24	4.39	4.30	4.28

is essential to obtain an accurate description. For heavier counterions, it is impossible to describe the data with the classical PB cylinder model. The problem with the latter model is that the data show too much curvature, and the smaller curvature of the experimental data can be reproduced by including an appropriate Stern capacitance. These observations are in contradiction with the assertion of some authors that the PB cylinder model can describe the charging data of PAA with for Na^+ as counterions [12–15]. This apparent discrepancy can be reconciled by realizing that our data span an unusually wide range of ionic strengths, while a much more limited window has been studied formerly. The latter data can be more easily reconciled with the cylinder PB model.

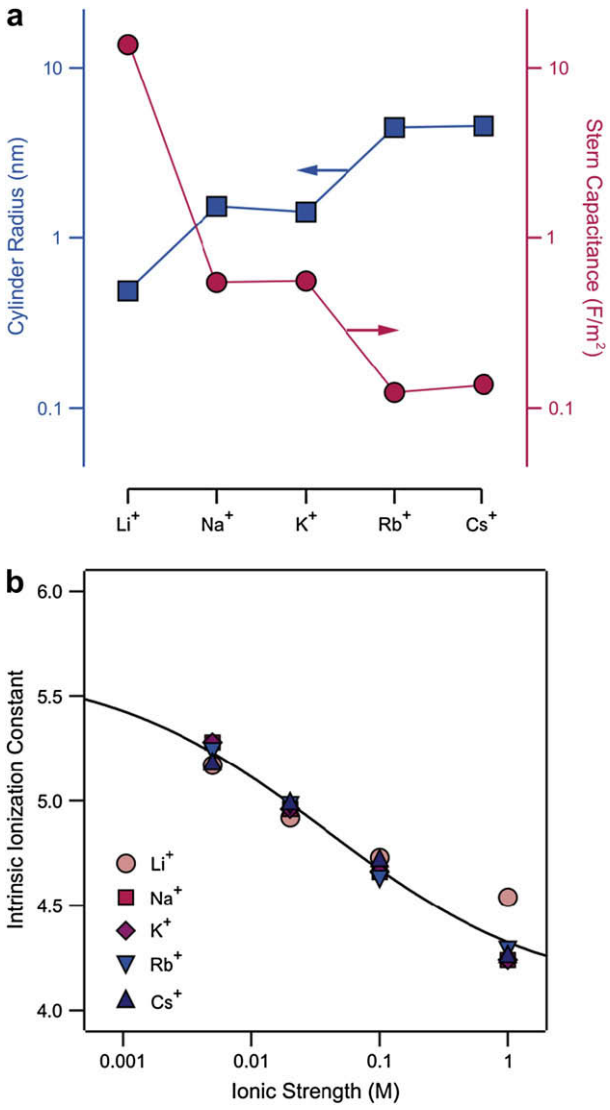

Fig. 5. Summary of fitted model parameters. (a) Cylinder radius and Stern capacitance for different counterions (Table 1). (b) Intrinsic ionization constant pK of the uncharged polymer as a function of the ionic strength (Table 2). The solid line represents the Davies-like Equation (8).

Our interpretation based on the cylinder Stern model reveals interesting trends with the mass of the alkali metal ions. Fig. 5a indicates that the fitted cylinder radius increases from about 0.5 nm about by a factor of ten. The reverse trend is observed for the Stern capacitance. The capacitance is reported normalized per unit area, but the same trend is observed when this quantity is normalized per unit length. Both effects can be explained qualitatively with the increasing ionic radii of the cations. For a plate capacitor, the capacitance is given by the relation

$$C_S = \frac{\varepsilon\varepsilon_0}{d} \tag{7}$$

where d is the distance between the plates. When interpreting this distance as the ionic radius, the Stern capacitance will decrease with increasing ionic radius. At the same time, the cylinder radius will increase. This situation is schematically depicted in Fig. 1c. The same trends are found when one used the appropriate expressions for a cylindrical capacitor. These trends are equally recovered from our data (see Fig. 5a). At this point, however, we are unable to provide a quantitative interpretation, especially for the similar behavior of the cations Na^+ and K^+ on one hand, and of the cations Rb^+ and Cs^+ on the other. The ionic radii increase from Li^+ to Cs^+ from 0.07 to 0.17 nm, but the increase in the fitted cylinder radius is much larger. Eventually, the conformation of the chain varies with different counterions. The discrepancy could be further related to the fact that cylinder Stern model is based on continuum PB theory, which is only approximate for highly charged systems [15,24,25].

Based on the molecular structure, one expects a mean axial distance between the charges of about $b \simeq 0.25$ nm. While a similar description of the data is possible with this value, one obtains unrealistically large values of cylinder radii, especially for the heavier counterions. The axial distance of $b = 0.5$ nm appears more realistic, and indicates that the distance between the carboxylic groups within the chain is larger, probably due to its syndiotactic structure. Larger axial distances lead to unrealistically small cylinder radii in the fits, especially for the Li^+ data. These distances are negligible with respect to the persistence length of PAA. Based on viscosity measurements and small angle X-ray scattering persistence lengths in the range 2–50 nm were reported for PAA and found to increase with decreasing ionic strength [32–34]. These two length scales become comparable only at the highest ionic strengths. Under these conditions the site–site interactions are weak and the details of the models are irrelevant.

Another interesting observation from the present experiments is related to the intrinsic ionization constants pK of the unchanged chains. This value can be obtained by extrapolation of pK_{eff} for $\alpha \to 0$. The present data clearly demonstrate that this value decreases with the ionic strength. For this reason, an accurate description of the data is impossible to obtain by assuming a common value of the constant pK for all ionic strengths, as done previously. Fig. 5b shows the decrease of the fitted intrinsic ionization constants pK with the ionic strength as expected for an acidic group [35]. The dependence on the ionic strength I can be approximately described with a Davies-like equation

$$\mathrm{p}K = \mathrm{p}K_0 - \frac{A\sqrt{I}}{1 + B\sqrt{I}} \tag{8}$$

with the parameters $\mathrm{p}K_0 \simeq 5.65$, $A \simeq 8.0\ \mathrm{M}^{-1/2}$ and $B \simeq 5.1\ \mathrm{M}^{-1/2}$. It is instructive to compare the intrinsic ionization constant extrapolated to zero ionic strength pK_0 with the corresponding values of low molecular mass aliphatic carboxylic acids. For propionic acid one has $\mathrm{p}K_0 \simeq 4.87$, while the two macroscopic constants of succinic acid of 4.21 and 5.64 lead to an intrinsic constant of $\mathrm{p}K_0 \simeq 4.51$ [15,36]. The substantially higher value of PAA suggests the importance of the low dielectric constant environment induced by the polyelectrolyte backbone. The type of counterion has little influence on the observed intrinsic constant, which further indicates weak specific ion binding of the alkali metal counterions. However, specific interactions with PAA were reported with multivalent ions or complexing monovalent ions (e.g., Ag^+) [16–19].

4. Conclusion

Charging of poly(acrylic acid) (PAA) in the presence of alkali metal counterions was studied by potentiometric titration. The charging depends systematically on the nature of the counterion and can be modeled with a cylinder Stern model quantitatively. With increasing mass of the alkali metal ion, the cylinder radius increases and the Stern capacitance decreases. Similarly to weak acids of low molecular mass, the intrinsic ionization constants for the uncharged polymer decrease with ionic strength.

Acknowledgement

Financial support from the Swiss National Science Foundation and the University of Geneva is acknowledged.

References

[1] Dautzenberg H, Jaeger W, Kotz J, Philipp B, Seidel C, Stscherbina D. Polyelectrolytes: formation, characterization and application. New York: Hanser Publishers; 1994.
[2] Bolze J, Peng B, Dingenouts N, Panine P, Narayanan T, Ballauff M. Langmuir 2002;18:8364–9.
[3] Liu Q, Wang Q, Xiang L. Appl Surf Sci 2008;254:7104–8.
[4] Tobori N, Amari T. Colloids Surf A 2003;215:163–71.
[5] Currie EPK, Sieval AB, Fleer GJ, Cohen Stuart MA. Langmuir 2000;16:8324–33.
[6] Wittemann A, Haupt B, Ballauff M. Phys Chem Chem Phys 2003;5:1671–7.
[7] Petrov AI, Antipov AA, Sukhorukov GB. Macromolecules 2003;36:10079–86.
[8] Kim HG, Lee JH, Lee HB, Jhon MS. J Colloid Interface Sci 1993;157:82–7.
[9] Guo X, Ballauff M. Langmuir 2000;16:8719–26.
[10] Gregor HP, Luttinger LB, Loebl EM. J Am Chem Soc 1954;76:5879–80.
[11] Sakurai M, Imai T, Yamashita F, Nakamura K, Komatsu T, Nakagawa T. Polym J 1993;25:1247–55.
[12] Nagasawa M, Murase T, Kondo K. J Phys Chem 1965;69:4005–12.
[13] Kawaguchi Y, Nagasawa M. J Phys Chem 1969;73:4382–4.
[14] Borkovec M, Koper GJM, Piguet C. Curr Opin Colloid Interface Sci 2006;11:280–9.
[15] Borkovec M, Jonsson B, Koper GJM. Colloid Surf Sci 2001;16:99–339.
[16] Miyajima T, Mori M, Ishiguro S. J Colloid Interface Sci 1997;187:259–66.
[17] David C, Companys E, Galceran J, Garces JL, Mas F, Rey-Castro C, et al. J Phys Chem B 2007;111:10421–30.
[18] Porasso RD, Benegas JC, van den Hoop MAGT. J Phys Chem B 1999;103:2361–5.
[19] Montavon G, Bouby M, Huclier-Markai S, Grambow B, Geckeis H, Rabung T, et al. J Colloid Interface Sci 2008;327:324–32.
[20] Kitano T, Kawaguchi S, Ito K, Minakata A. Macromolecules 1987;20:1598–606.
[21] de Groot J, Koper GJM, Borkovec M, de Bleijser J. Macromolecules 1998;31:4182–8.
[22] Smits RG, Koper GJM, Mandel M. J Phys Chem 1993;97:5745–51.
[23] Borkovec M, Koper GJM. J Phys Chem 1994;98:6038–45.
[24] Ullner M, Jonsson B. Macromolecules 1996;29:6645–55.
[25] Ullner M, Woodward CE. Macromolecules 2000;33:7144–56.
[26] Adamczyk Z, Bratek A, Jachimska B, Jasinski T, Warszynski P. J Phys Chem B 2006;110:22426–35.
[27] Joyce DE, Kurucsev T. Polymer 1981;22:415–7.
[28] Garces JL, Koper GJM, Borkovec M. J Phys Chem 2006;110:10937–50.
[29] Uyaver S, Seidel C. Europhys Lett 2003;64:536–42.
[30] Hiemstra T, de Wit JCM, van Riemsdijk WH. J Colloid Interface Sci 1989;133:105–17.
[31] Kobayashi M, Juillerat F, Galletto P, Bowen P, Borkovec M. Langmuir 2005;21:5761–9.
[32] Tricot M. Macromolecules 1984;17:1698–704.
[33] Mylonas Y, Staikos G, Ullner M. Polymer 1999;40:6841–7.
[34] Taylor TJ, Stivala SS. J Polym Sci Part B Polym Phys 2003;41:1263–72.
[35] Perrin DD, Dempsey B, Serjeant EP. pKa prediction for organic acids and bases. New York: Chapman and Hall; 1981.
[36] Martell AE, Smith RM. Critical stability constants. New York: Plenum Press; 1982.